

UNCLASSIFIED

2

SECURITY				<b>T DOCUMENTATION PAGE</b>			
1a. REPR <b>AD-A208 864</b>				1b. RESTRICTIVE MARKINGS			
2a. SECL				3 DISTRIBUTION / AVAILABILITY OF REPORT Approved for public release; distribution unlimited			
2b. DECLASSIFICATION / DOWNGRADING SCHEDULE				5. MONITORING ORGANIZATION REPORT NUMBER(S) <b>AFOSR-TR-89-1705</b>			
4 PERFORMING ORGANIZATION REPORT NUMBER(S)				7a. NAME OF MONITORING ORGANIZATION Air Force Office of Scientific Research/NL			
6a. NAME OF PERFORMING ORGANIZATION Oregon State University		6b. OFFICE SYMBOL (If applicable)		7b. ADDRESS (City, State, and ZIP Code) Building 410 Bolling AFB, DC 20332-6448			
6c. ADDRESS (City, State, and ZIP Code) PO Box 1086 Corvallis, OR 97339		8a. NAME OF FUNDING / SPONSORING ORGANIZATION AFOSR		8b. OFFICE SYMBOL (If applicable) NL		9. PROCUREMENT INSTRUMENT IDENTIFICATION NUMBER AFOSR 86-0076	
8c. ADDRESS (City, State, and ZIP Code) Building 410 Bolling AFB, DC 20332		10 SOURCE OF FUNDING NUMBERS		PROGRAM ELEMENT NO. 61102F		PROJECT NO. 2312	
				TASK NO. A1		WORK UNIT ACCESSION NO.	
11. TITLE (Include Security Classification) Unclassified Variability and Chaos: Neurointegrative Principles in Self-organization of Motor Patterns							
12. PERSONAL AUTHOR(S) G.J. Mpitsos, H.C. Creech, C.S. Cohan and M. Mendelson							
13a. TYPE OF REPORT Publications		13b. TIME COVERED FROM 1/10/86 TO 1/14/89		14. DATE OF REPORT (Year, Month, Day) March 15, 1989		15. PAGE COUNT 29	
16. SUPPLEMENTARY NOTATION In: Dynamic Patterns in Complex Systems. J.A.S. Kelso, A.J. Mandell, & M.F. Shessinger, eds World Scientific Pub 1988 pp 162-190							
17. COSATI CODES			18. SUBJECT TERMS (Continue on reverse if necessary and identify by block number)				
FIELD	GROUP	SUB-GROUP	Variability, Self-organization, mechanisms, neurocircuits, Chaos, Adaptive behavior,				
19. ABSTRACT (Continue on reverse if necessary and identify by block number)  See reverse							
20. DISTRIBUTION / AVAILABILITY OF ABSTRACT <input checked="" type="checkbox"/> UNCLASSIFIED/UNLIMITED <input type="checkbox"/> SAME AS RPT <input type="checkbox"/> DTIC USERS				21. ABSTRACT SECURITY CLASSIFICATION Unclassified			
22a. NAME OF RESPONSIBLE INDIVIDUAL Dr. William O. Berry				22b. TELEPHONE (Include Area Code) (202) 767-5021		22c. OFFICE SYMBOL NL	

**DTIC**  
**ELECTE**  
**JUN 06 1989**  
**S E D**

89 6 06 102

In this chapter we discuss the possibility that variability may be a central feature of self-organizing processes. We suggest that variability may be inherently part of the mechanisms by which adaptive "neurocircuits" emerge, and contrast such functional neurocircuits against definitions involving anatomical or dynamical structures which the self-organizational definition both contains and supercedes. The experimental work focuses on an invertebrate animal, the sea slug, *Pleurobranchaea californica*, which has a rich behavioral repertoire of buccal/oral behaviors, and a relatively simple nervous system containing identifiable neurons. We present evidence from work on a set of 20 neurons, which we refer to as BCNs (buccal-cerebral neurons), that communicate between the buccal ganglion and cerebral ganglion. These neurons are crucial for generating all buccal/oral behaviors, and provide an advantageous source of experimental material for inquiring into the self-organization of group activity. Variability in the activity of the BCNs, and in the motoneurons that they drive, is attributable to low-dimensional chaos, as shown by: 1) autocorrelation functions; 2) correlation analysis of phase portrait dimensions; 3) calculation of Lyapunov exponents; and 4) the structure of 10 maps of Poincaré sections. These findings indicate that some variability may arise from the same mechanisms that generate the patterned activity: i.e., that the observed variations are not noise that is superimposed on the code underlying a behavior, but rather that they constitute the code itself. We discuss the findings with respect to the role of sensory feedback in the production of adaptive behavior of animals as they interact with complex and often unpredictable environments, and we suggest that chaotic neural activity provides a means for the nervous system to create new informational space rendering animals more stably adaptable in such changing environments.

Accession For	
NTIS GRA&I	<input checked="" type="checkbox"/>
DTIC TAB	<input type="checkbox"/>
Unannounced	<input type="checkbox"/>
Justification	
By	
Distribution/	
Availability Codes	
Dist	Avail and/or Special
A-1	



VARIABILITY AND CHAOS: NEUROINTEGRATIVE PRINCIPLES IN SELF-ORGANIZATION  
OF MOTOR PATTERNS<sup>1</sup>

G. J. Mpitsos, H. C. Creech, C. S. Cohan<sup>2</sup>, and M. Mendelson<sup>3</sup>  
Oregon State University  
M.O. Hatfield Marine Science Center  
Newport, OR 97365  
USA

ABSTRACT AFOSR-TR-89-0705

In this chapter we discuss the possibility that variability may be a central feature of self-organizing processes. We suggest that variability may be inherently part of the mechanisms by which adaptive "neurocircuits" emerge, and contrast such functional neurocircuits against definitions involving anatomical or dynamical structures which the self-organizational definition both contains and supercedes. The experimental work focuses on an invertebrate animal, the sea slug, *Pleurobranchaea californica*, which has a rich behavioral repertoire of buccal/oral behaviors, and a relatively simple nervous system containing identifiable neurons. We present evidence from work on a set of 20 neurons, which we refer to as BCNs (buccal-cerebral neurons), that communicate between the buccal ganglion and cerebral ganglion. These neurons are crucial for generating all buccal/oral behaviors, and provide an advantageous source of experimental material for inquiring into the self-organization of group activity. Variability in the activity of the BCNs, and in the motoneurons that they drive, is attributable to low-dimensional chaos, as shown by: 1) autocorrelation functions; 2) correlation analysis of phase portrait dimensions; 3) calculation of Lyapunov exponents; and 4) the structure of 1D maps of Poincaré sections. These findings indicate that some variability may arise from the same mechanisms that generate the patterned activity: i.e., that the observed variations are not noise that is superimposed on the code underlying a behavior, but rather that they constitute the code itself. We discuss the findings with respect to the role of sensory feedback in the production of adaptive behavior of animals as they interact with complex and often unpredictable environments, and we suggest that chaotic neural activity provides a means for the nervous system to create new informational space rendering animals more stably adaptable in such changing environments. *ADJ*

*(is discuss)*

INTRODUCTION

Self-organization represents the ability of groups of individuals to act "cooperatively" [7,12,16,17,20,53]. These groups consist of relatively autonomous individuals, each acting nonlinearly and usually having information of what only part of the group is doing. Some individuals may have more persuasive powers than others, but given the information concerning a single individual, an observer could not determine the behavior nor future action of the group.

Hidden in the above account is the role that variability may have in establishing cooperative behavior. In neural systems, computer simulation studies have shown that a network of interconnected elements can produce different patterns of activity, depending of the

<sup>1</sup>This work was supported by grant AFOSR-86-0076.

<sup>2</sup>Present address: Department of anatomy, SUNY, Buffalo, NY 14226.

<sup>3</sup>Present address: Department of Family Medicine, University of Washington, Seattle, WA 98195, and Tacoma Family Medicine.

parametric state of the network [18,37,44]. In the same way, recent neurophysiological studies on simple systems indicate that the same population of identifiable neurons can produce different patterns of activity, depending on differences in sensory inputs or neurohumoral factors [11,13,31,42,47]. Because of the high degree of parallel interconnections among neurons in most nervous systems, it has become obvious that it is not possible to predict how the system will work dynamically by simply looking at the architecture of the neurocircuit; i.e., to determine the functional characteristics of any given neuron or of a group of neurons, it is necessary to examine the system during its temporal expression.

However, while the attribute of being parallel implies dynamical, it does not necessarily account for self-organization adequately. A functional neurocircuit arising from parallel networks may require dynamics in order to appear, but if the temporal characteristics and final result of the dynamics are always the same, the definition of self-organization has not progressed much beyond the original one in which the information for a motor pattern or a behavior resides in the neuroanatomy itself. This is not to say that the framework of anatomical, physiological, and neurohumoral factors are not essential. But while changes in these frameworks, such as synaptic modifications arising from associative learning or changes in hormone levels, may lead to different behaviors, they do not necessarily speak directly to the issue of self-organization. The central issue, we believe, is to account for the process by which both similar and different behaviors emerge from the same underlying framework, and how this framework can produce the same behavior in different ways. Thus, at least conceptually, self-organization seems to be tied to variability.

Observations of extensive variations in behavioral and neural responses have led us to suggest that variability may be an inseparable part of the mechanisms generating motor patterns rather than representing extraneous noise [38,39]. This is to say that variation is not noise riding on the neural code, but rather that the variation resides within the code itself. One of the simplest examples of this relationship between code and variation is the logistic equation,  $X_{n+1} = A(1-X_n)X_n$ , where each successive value  $X_{n+1}$  is generated from the previous value  $X_n$  [32]. For values of the constant  $A$  just below 4, the equation gives unpredictable results: although there is no noise in the equation, given a solution to the equation for a particular value of  $X$ , the probability of predicting the solution at some future value quickly decreases. This sensitivity to initial conditions is a characteristic feature of chaotic systems; the systems follow deterministic laws such as the logistic equation, but the behavior of the systems is not predictable into the future.

This inseparable connection between signal and noise has led us to inquire into the possibility that variability in our experimental system may also be chaotic. Our approach has been to take advantage of the technical amenities of invertebrate animals in which it is possible

to identify specific neurons or small groups of neurons repeatedly from one animal to another [41]. In order to understand how adaptive behavior arises in whole animals, such groups of neurons should have a central role in generating behaviors, but the number of neurons in the group should be small enough to permit a quantitative analysis of all of their responses. In broad terms, the experimental problem may best be viewed as an inquiry into the process by which an individual affects the functioning group, and, in turn, how the group affects the individual. In the present paper we begin to address this problem by examining the temporal characteristics of activity in individual neurons during the production of repetitive activity arising from coordinated interactions in the group of neurons to which the neuron in question belongs.

### THE EXPERIMENTAL SYSTEM

The sea slug *Pleurobranchaea californica*, a marine gastropod mollusc, produces many different buccal/oral behaviors that outwardly seem to have similar repetitive movements. Some of the most interesting of these behaviors consist of: several components of feeding, such as biting, ingestion, and swallowing movements; an obvious, active form of regurgitation; a food-rejection behavior by which the animal sequentially expels unwanted substances from the mouth in a fashion resembling a reverse of the bite-ingestion phases of feeding; and self- and interanimal gill grooming. An example of a feeding response appears in Fig. 1.

The nervous system of this animal consists of four major ganglia and several minor ones. Of the major structures, there are two pedal ganglia, one for each of half of the foot; one buccal ganglion which drives the opening and closing of the jaws and controls the movements of the radula, a structure which is analogous to a tongue; and a cerebral ganglion (brain) which innervates the mouth, lips, and the anterior regions of the head. Connectives (cables of nerve axons) convey information between specific ganglia.

In *Pleurobranchaea*, as in many other invertebrate animals and in some vertebrates, many neurons can be visually or physiologically identified either individually or in small groups [8,13,24,41,42,45,47]. Despite the relative simplicity of these animals, hundreds or thousands of neurons may become active in the production of a given behavior. However, although there are approximately 10,000 neurons in the nervous system of *Pleurobranchaea*, a peculiarity in its neuroanatomy (and probably in the nervous systems of many of its cousins) significantly reduces the number of neurons one needs to consider in order to inquire into self-organization. For proper coordination to occur between the movements of the jaws and mouth in *Pleurobranchaea*, it is necessary that the brain receive information about activity in the buccal ganglion (Fig. 2). It so happens that there is only one group of 15-20 neurons in each buccal hemiganglion that can perform this information-carrying capacity. We refer to them as BCNs

(buccal-cerebral neurons), and they, along with one giant neuron, are the only neurons that send axons from the buccal ganglion to the brain.

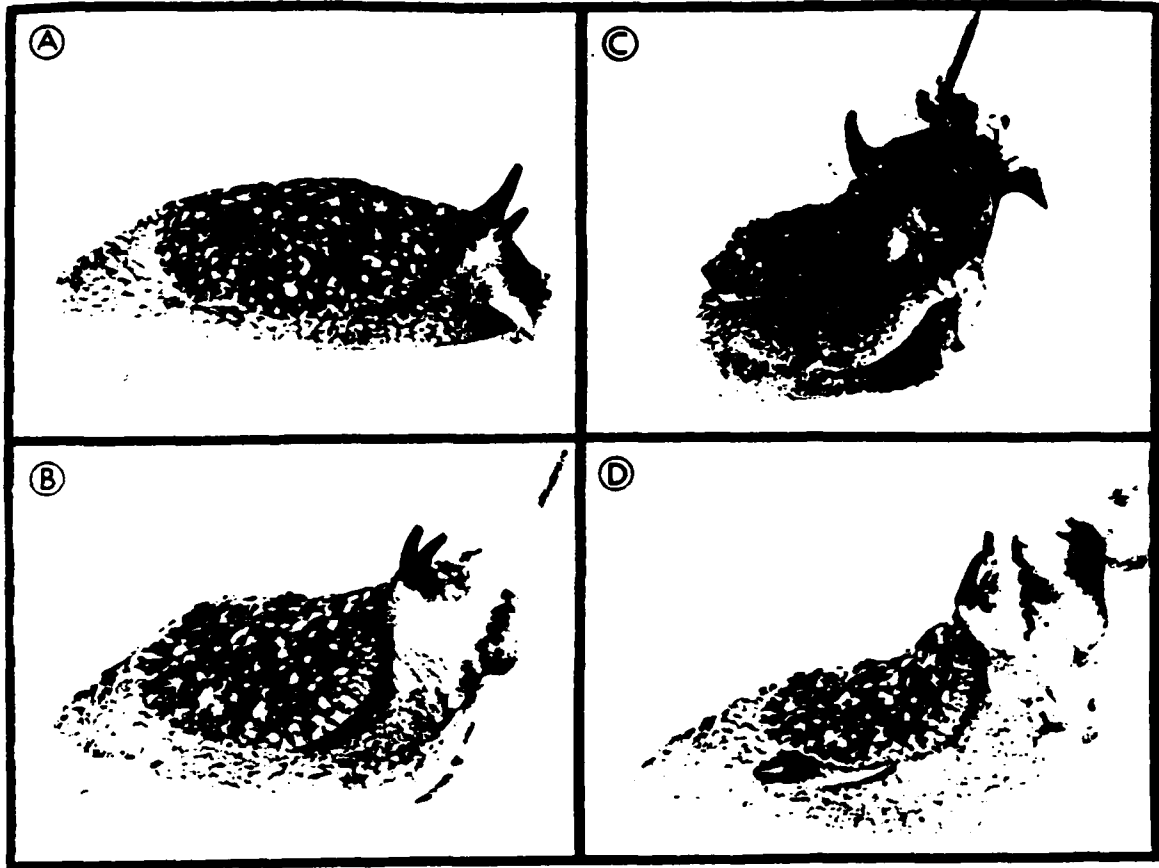


**Figure 1:** Photographs of the carnivorous mollusc *Pleurobranchaea* (A) locomoting from left to right. (B-D) increasing responses to food descending from a small tube at the upper right. Note progressive extension of the proboscis and opening of the mouth in (C). Response in (D) occurred within a fraction of a second from a starting posture as in (A). Cowcatcher-like structure lying over the proboscis is a sensory oral veil for detecting chemical and mechanical stimuli. Pair of upwardly directed objects are rhinophores which perform chemosensory functions. The unpaired gill is on the right side; best seen in (C) and (D). (from Mpitsos, Collins, and McClellan [40]).

It is relatively easy to record intracellularly from individual neurons, and extracellularly from the nerve bundles that communicate between the various ganglia. Because of the anatomical separation of the ganglia, it is possible either to examine local effects arising from activity within a group of neurons or within a single ganglion by severing the connectives, or to examine the interactions between groups of neurons by leaving the connectives intact. Such work has shown that the BCNs have a multiplicity of functions, but their most important feature is that the functional attributes of a given neuron, or of the group as a whole, emerge from the

interrelationship or context of firing among all the coactive neurons [39]. Moreover, the firing of individual neurons and of the group is quite variable, as are the behaviors that these neurons help to form and regulate [38]. The BCNs intercommunicate among themselves, converge and diverge onto interneurons and motoneurons in the brain and buccal ganglion, they receive feedback from by the motoneurons that they drive [39], and they feed back onto the interneurons that drive them [14]. As such findings show, the neuroanatomic architecture of *Pleurobranchaea* is designed for a high degree of parallel processing.



**Figure 2:** Brain (top panel: dorsal view); buccal ganglion (bottom panel, ventral view). Small dark objects are neurons that have been filled with a black precipitate (cobalt sulfide) for better visualization. Cells in the brain are motoneurons that innervate the mouth and lips. Cells in the buccal ganglion are BCNs, many of which contact brain motoneurons either monosynaptically or polysynaptically. Not shown is that each buccal hemiganglion connects with the corresponding half of the brain by means of a long cerebral-buccal nerve connective (CBC). Magnification: brain (22X); buccal ganglion (32X).

As in most invertebrate animals, the *Pleurobranchaea* nervous system functions well after being removed from the rest of the animal. Such isolated nervous systems can generate two characteristic types of motor patterns relating to different behaviors, one relating to the swallowing phase of feeding, and the other relating to the active phase of regurgitation (see Mptsos and Cohan [38,39] for a critical discussion). In the following sections we examine first the motor pattern relating to feeding and then discuss an example relating to regurgitation.

#### COOPERATIVITY AND VARIABILITY IN SELF-ORGANIZING PROCESSES

Among their various functions, the BCNs generate the cyclical rhythm for opening and closing the jaws. This rhythmic activity is shown in Fig. 3 as sequences of bursts in buccal ganglion nerve root R3 which contains motoneurons that activate muscles for closing the jaws,

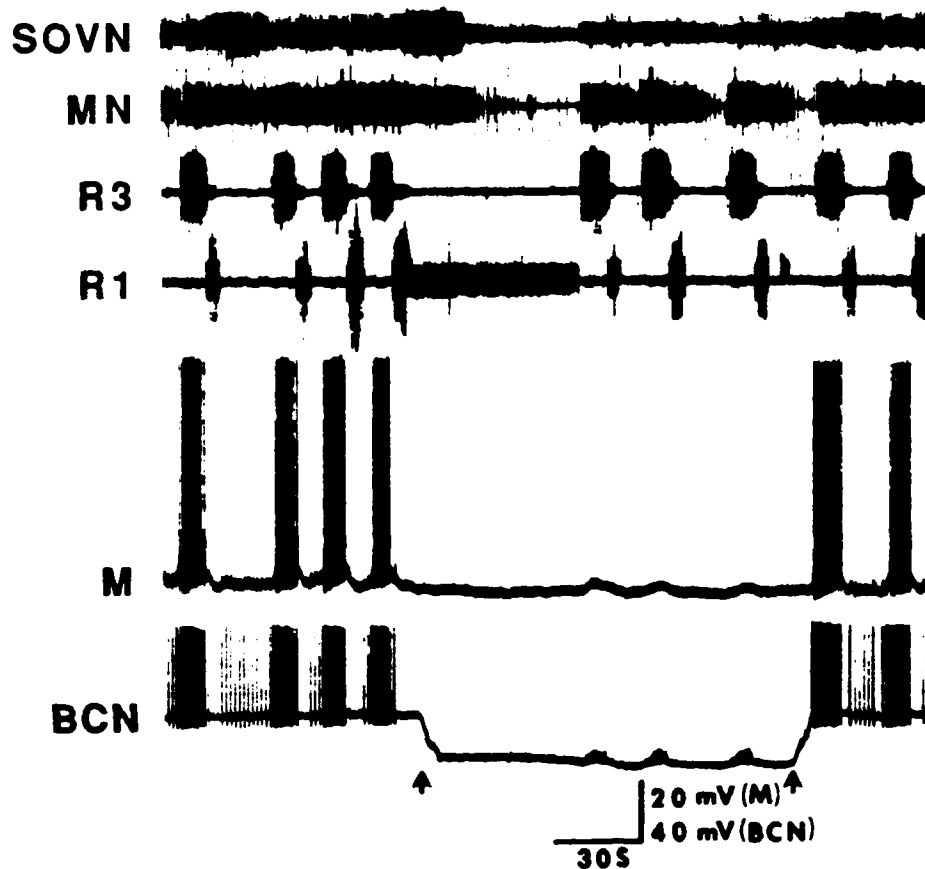


**Figure 3:** Functional "cooperativity" following perturbation of patterned activity. Top four traces are extracellular recordings from nerve roots, each containing activity of many motoneuron axons. Bottom two traces are intracellular recordings from a motoneuron (M) and a BCN. Removal of the BCN by hyperpolarizing it (between arrows) caused cessation of all activity, but the activity in the rest of nervous system eventually recovered despite the fact that the hyperpolarization forced the BCN to remain quiescent. Activity here, as in all physiological records shown below, was elicited by tonic electrical stimulation of a sensory root of the buccal ganglion. SOVN: brain nerve root innervating the oral veil and anterior mouth. MN: brain nerve

root innervating the mouth; contains axon of M. R3: buccal ganglion nerve root containing motoneurons for closing jaws. R1: buccal ganglion root containing motoneurons for opening jaws. (From Mpitsos and Cohan [39]).

and in root R1 which contains motoneurons that activate muscles for opening the jaws. As a group, the BCNs have heterogeneous effects on the generation of patterned activity. Figure 3 shows a BCN that initially had a strong effect. Removal of this neuron from the circuit (by passing hyperpolarizing current through the intracellular recording electrode) immediately stopped all cyclical activity in motoneuron (M), in buccal roots R3 and R1, and in brain nerve roots SOVN and MN. After about 60 sec, the pattern reestablished itself, despite the fact that the BCN was still hyperpolarized. With each cycle in the reestablished pattern the membrane potential of the BCN and MN exhibited small excitatory synaptic bumps originating from parallel inputs from the BCNs and other newly activated neurons. Release of the BCN from hyperpolarization (second arrow in Fig. 3) also released the motoneuron but had little effect on the pattern of activity in the rest of the nervous system.

Another example of changeable function in single neurons appears in Fig. 4 which shows the effect of the history of activity in the nervous system on subsequent activity in single neurons. Sections A and B of Fig. 4 each contain a motor pattern relating to the swallowing phase of feeding. However, in Fig. 4A the BCN and motoneuron fired most actively in phase with the R1 portion of the buccal cycle, whereas in Fig. 4B they fired in phase with the R3 portion. The only difference between these two recording situations was that in Fig. 4A the activity was recorded soon after the nervous system had generated a regurgitation motor pattern, whereas in Fig. 4B the activity was recorded after the nervous system had been generating the pattern relating to swallowing behavior.

The recordings in Figs. 3 and 4 illustrate two important interrelated features of cooperativity and self-organization: 1) Patterns of responses can be established in different ways, and 2) individual neurons can exhibit different functional properties within similar patterns. In Fig. 3 the BCN initially had a strong effect in pattern generation, but then it lost this effect when other BCNs reinstated the pattern. In Fig. 4 the BCN and motoneuron remained active throughout, but completely changed their phase of activity as a consequence of the preceding activity.

Both of these examples are extreme cases of variability. Closer inspection of the traces in Figs. 3 and 4 shows that there were many instances of relatively small variations. For example, the number of action potentials in the bursts of R1 in Fig. 3, and the number of action potentials in the BCN and motoneuron in Fig. 4, differed from one burst to another. We believe that the more extreme forms of variability arise from the same nonlinear dynamics that produce the small variations. Some of these smaller variations are examined quantitatively in the following section.

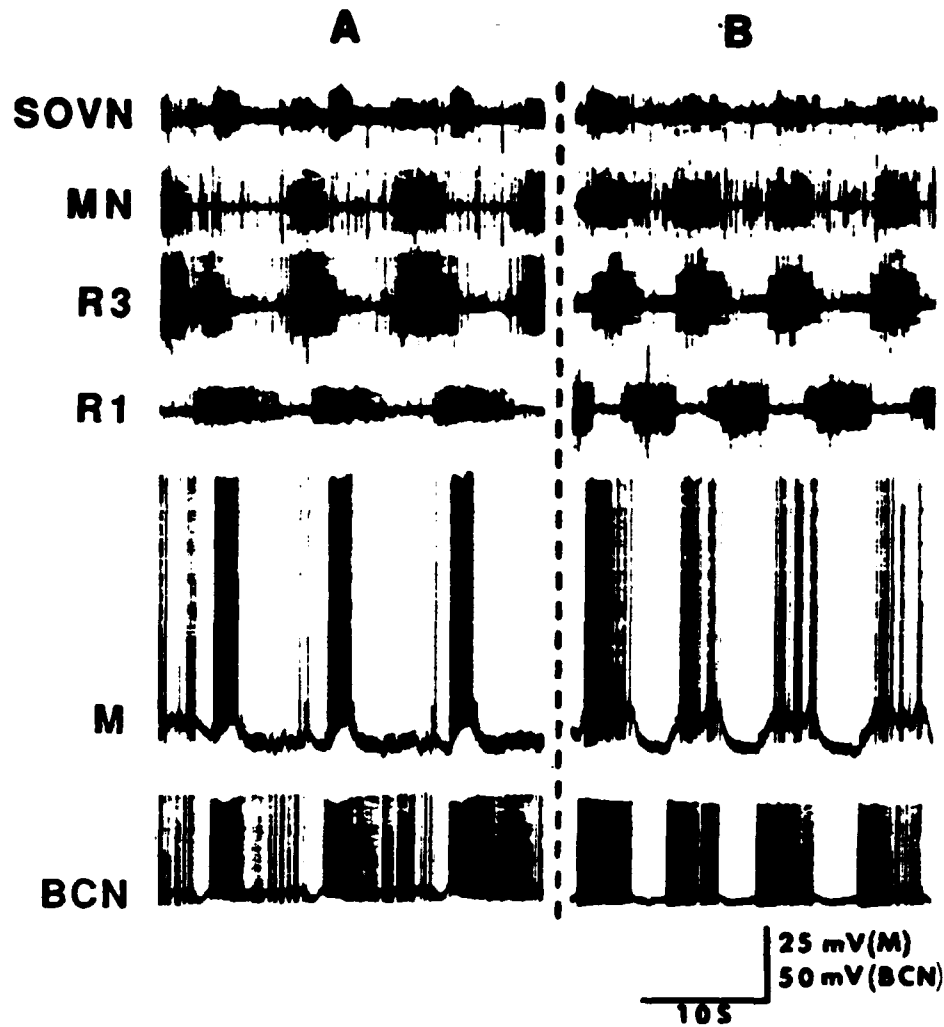


**Figure 4:** History of activity in the nervous system affects the way in which activity among neurons self-organizes to produce similar motor patterns. Same captions as in Fig. 3; different M and BCN. Note that the BCN and M were most active during the R1 phase of the buccal cycle in (A) whereas they were most active during the R3 phase in (B). (From Mpitsos and Cohan [39]).

#### DYNAMICS OF FIRING IN SINGLE NEURONS DURING PATTERNED ACTIVITY

##### *Interpolation of Time Series*

The time series of intracellular responses of BCNs and motoneurons (as in Figs. 3 and 4) were first recorded on FM tape. Selected portions were then played back and digitized at 1K Hz for computer analysis. The rate of digitization was adequate for analysis of the 10 to 15 msec action potential durations that are typical of molluscan neurons. As in Figs. 3 and 4, the activity described below was activated by electrically stimulating the stomatogastric nerve which innervates the esophagus and carries chemosensory information to the buccal ganglion. The

stimuli were presented at 1 Hz, and at an electrical current strength near the threshold for generating the bite-swallow motor pattern [see also 34-36,39].

To illustrate the analysis, we selected the activity of a brain motoneuron which received converging inputs from several BCNs. The motor pattern was about 168 sec long and contained 548 action potentials. Bouts of feeding in whole animals varies from several seconds to several minutes, and, therefore, the selected record was within the range of typical behavior in whole animals. At digitization rates of 1K Hz, the number of points in the 168 sec time series was too long for analysis on a typical laboratory microcomputer. In order to reduce the amount of data, we used the sequence of unequal intervals occurring between action potentials instead of the equally spaced samples in the digitized series. Longer patterns have been recorded from other neurons, but we chose the present ones so as to examine situations that physiologists may typically encounter in experimentation: i.e., the length of the data was representative of adaptive responses in whole animals; the data required compression, but, once compressed, the series was relatively short and contained few cycles of structured activity.

Analysis of time series composed of such unequally spaced spike intervals in BCNs and motoneurons in *Pleurobranchaea* have yielded evidence for low-dimensional chaos, as has been described for spontaneous activity in cat cortex [46]. We believe, however, that it is physiologically justifiable to convert the unequal time series into an equally spaced one by

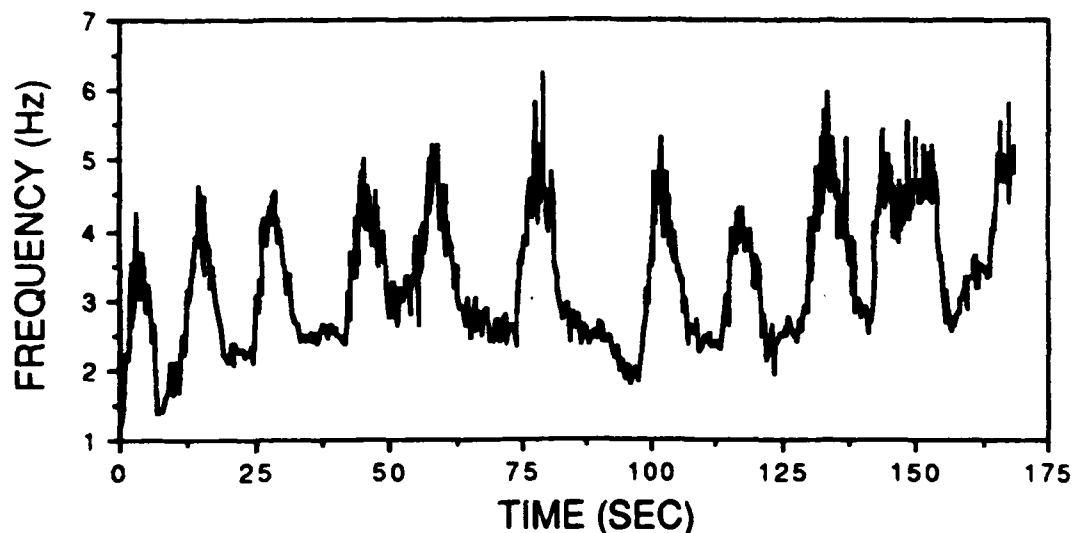


**Figure 5:** Firing frequency of a brain motoneuron during a 168 sec bout of the bite-swallow motor pattern. Frequency represents the reciprocal of the time between a spike in the motoneuron and the preceding spike. Data shown here is uninterpolated. For subsequent analyses, a variety of interpolation rates were used. Major criterion for effective interpolation was to reproduce all aspects of the shape in the uninterpolated series.

interpolation. First, it is a relatively safe assumption to make that the frequency of action potentials arriving at a synapse carries the code of the information in the input neuron's activity. Figure 5 shows the frequency series for the uninterpolated data obtained from the motoneuron described in the preceding paragraph. This series has three components: a slow trend in which the baseline frequency slowly increased throughout the series; 11 consecutive bursts of activity; and a high-frequency component which is superimposed on both the slow trend and the repeating bursts. Second, we propose that the shape or the envelope of such a frequency series, including initially all the components, contains the essential elements for reconstructing the information that one neuron conveys to another. Third, we propose that it is permissible to sample the series at equally spaced intervals as long as the interpolation rates retain the characteristics of the uninterpolated frequency function. This transformation to equally-spaced intervals allowed for the application of more analytical methods in examining the activity of single neurons than are available for unequally spaced intervals.

Because interpolation distributes the density of points evenly throughout the series, too low a rate underrepresented the high-frequency bursts. However, once we obtained good congruence between the shapes of the uninterpolated and interpolated series, the analyzed results remained stationary over a wide range of interpolation rates. In the present example, similar results were obtained using interpolation rates between 0.05 and 0.25 sec.

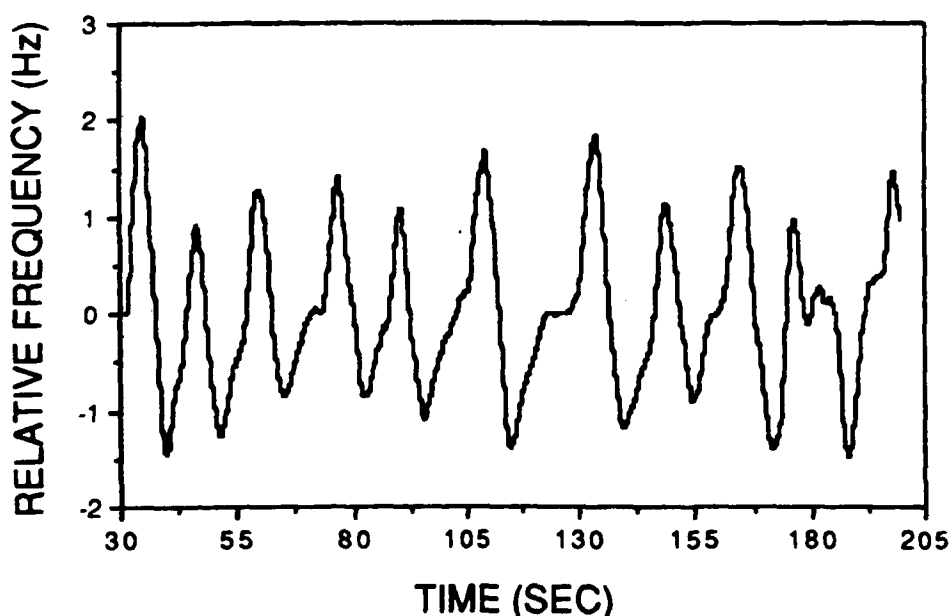


**Figure 6:** Same patterned activity as in Fig. 5, except that the activity was linearly interpolated at 0.10 sec intervals and passed through a filter having a high pass of 0.05 Hz, and a low-pass of 0.15 Hz.

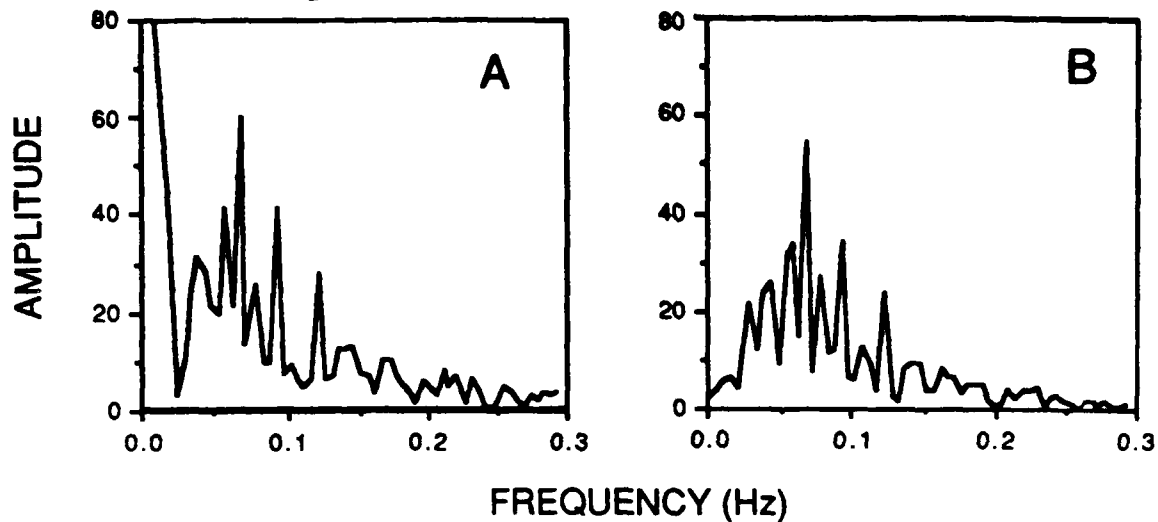


**Figure 7:** Amplitude spectra. (A) interpolated, unfiltered data. (B) interpolated and filtered data using a band pass of 0.05 to 0.15 Hz.

The amplitude spectra of the unfiltered and filtered series are shown in Fig. 7. Interestingly, the peaks are near but not exact multiples of one another. Examination of the data using different digitization and interpolation rates showed that the characteristics of the filtered and unfiltered spectra arose from the time series of the neuronal response rather than from the manipulations performed on the data. Moreover, when the pattern of activity spontaneously switched to another pattern representing the activity underlying regurgitation, the spectrum also changed, but, again, many of the peaks appeared to be close multiples of one another. Such spontaneous shifts in the pattern of neural activity are particularly interesting, and we shall return to them later in this chapter.

#### Autocorrelation Function

We examined autocorrelation functions for two reasons: 1) To obtain an indication of whether the activity was sensitive to initial conditions, i.e., whether the predictability of the activity decreased with increasing lags into its evolution. 2) To determine the appropriate lag for use in dimensional analysis.

The autocorrelation functions of the unfiltered time series slowly declined toward zero, reflecting the slow trend in the baseline frequency of Fig. 5, whereas the autocorrelation function of the filtered series quickly dropped to zero. Figure 8 shows that the autocorrelation function of the filtered series in Fig. 7B first crossed zero at a lag of 3.7 sec, and within 60 sec (approximately three cycles in the data of Fig. 6) the autocorrelation declined toward a more stable value near zero. Given the fact that the times series was repetitive and of relatively short duration, it is not surprising that harmonics appear at 75 and 150 sec, but the overall autocorrelation shows a consistent decline.

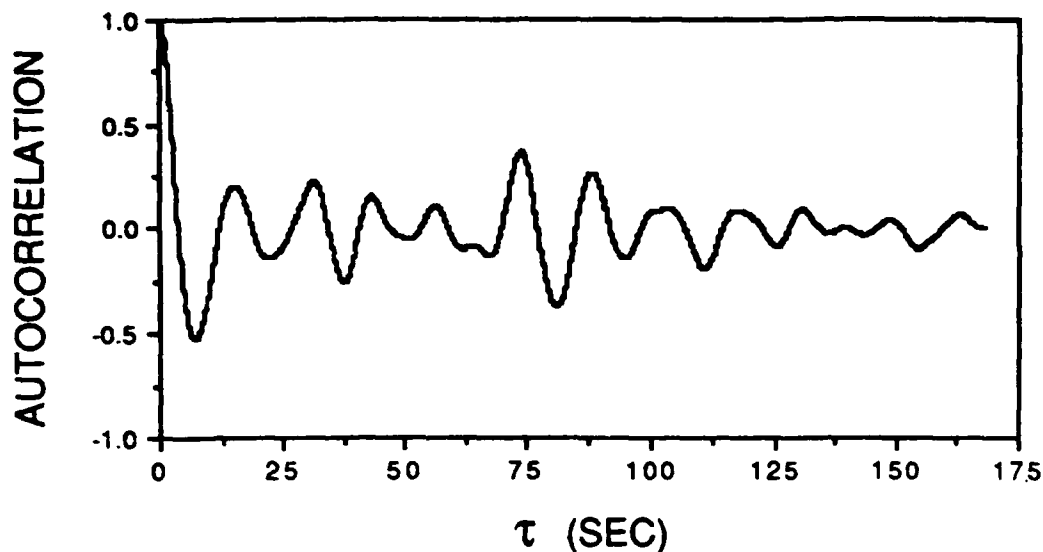


**Figure 8:** Normalized autocorrelation function of activity shown in Fig. 6.

#### Phase Portrait

From a time series of a single variable representing the combined effects of several processes, it is possible to obtain an indication of the dynamics of the activity and of the number of variables governing it. Following the work of Packard, Crutchfield, Farmer, and Shaw [43] and of Takens [54], we defined a multidimensional space by mapping the original frequency series  $f(t)$  along the  $x$  axis, then mapping the same data on the  $y$  axis after shifting it by a lag ( $\tau$ ), and on the  $z$  axis after a shift of  $2\tau$ . In  $d$ -dimensional space the procedure follows  $f(t+(d-1)\tau)$ , where  $\tau$  is an integer multiple of the sampling interval. The evolution of the time series through successive points in multidimensional space defines the trajectory of the activity, and the overall evolution defines the phase portrait. A 3-D view of the first six cycles in the time series of Fig. 6 is shown in Fig. 9. The trajectories begin at the upper right at the asterisk and progress clockwise and outward until reaching the  $f(t+2\tau)$  axis, then they swing in toward the origin and turn upward and outward again. The phase portrait resembles a bent coil. Even with so few cycles it is possible to see some divergence in the interrelationship of the trajectories, particularly at the sharp corner near the  $f(t+2\tau)$  axis. To construct this phase portrait and to conduct the analyses presented in subsequent sections, we used  $\tau = 3.7$  sec, or multiples of it, as determined from the first lag that generated a zero autocorrelation (Fig. 8). Karl Eugen Graf (Department of Clinical and Physiological Psychology, Tübingen) has obtained good congruence of results on EEGs using this method of selecting  $\tau$  and one based on mutual information theory (personal communication).

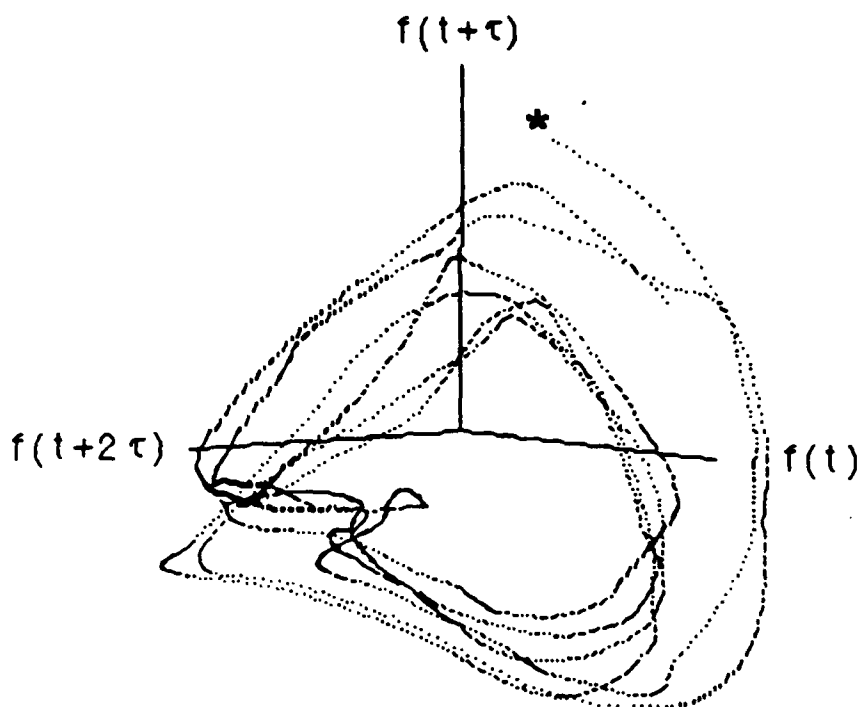


**Figure 9:** Phase portrait of activity shown in Fig. 6; for clarity, only the first six cycles are shown. The original series,  $f(t)$ , was mapped on the x-axis, and then successively shifted by a lag  $\tau$  on the y-axis and by  $2\tau$  on the z-axis. The  $\tau$  (3.7 sec) was selected from the first zero crossing of the autocorrelation function.

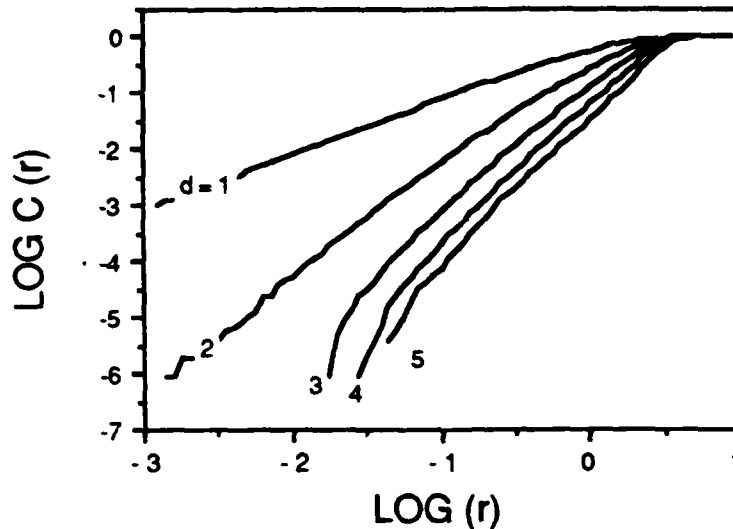
#### Correlation Dimension

Dimensional analyses provide an indication of two important features of time series: the number of dimensions ( $d$ ) that govern the phase space, and the topological dimension ( $n$ ) of the phase portrait, which denotes the dynamical nature of the time series. Following Grassberger and Procaccia [15], we defined an integral autocorrelation function:

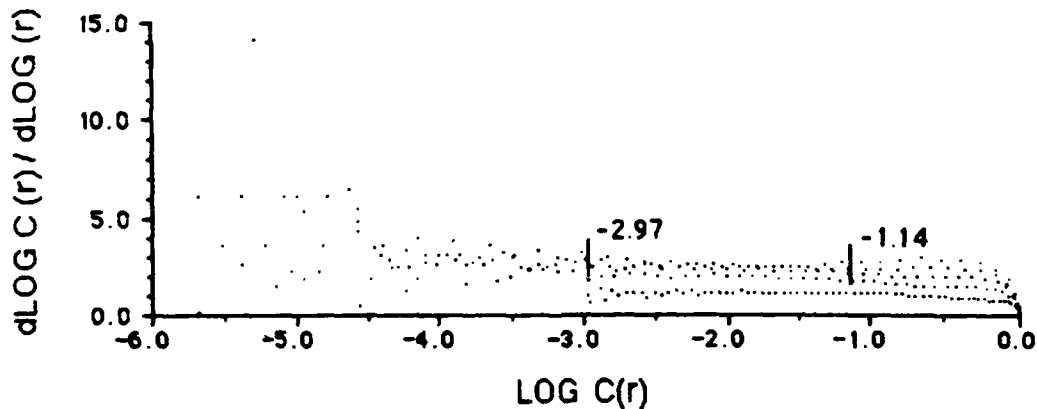
$$C(r) = \frac{1}{N^2} \sum_{\substack{i, j=1 \\ i \neq j}}^N \theta(r - |X_i - X_j|) \quad (1)$$

This algorithm selects a point  $X_i$  and measures the number of points  $X_j$  lying within a prescribed range of distances  $r$  until all  $N-1$  points of the series are counted. The function  $\theta$  excludes points lying outside each  $r$ . The process is then repeated by selecting another point as  $X_i$  for all  $N$  points. For small  $r$ ,  $C(r)$  scales as  $r^n$ . Thus,  $n$  may be obtained from the slopes of plots of  $\log C(r) = n \log(r)$ . The calculations are made for a series of embedding dimensions  $d$ : For random noise  $n$  scales linearly with increasing  $d$ ; i.e., noise fills all space as dimensions are

added, but in deterministic processes, the value of  $n$  levels off (saturates) after a certain  $d$ . Integer  $n$  values usually indicate predictable activity tending asymptotically toward some limit, whereas noninteger (fractal) values indicate chaotic activity [30].



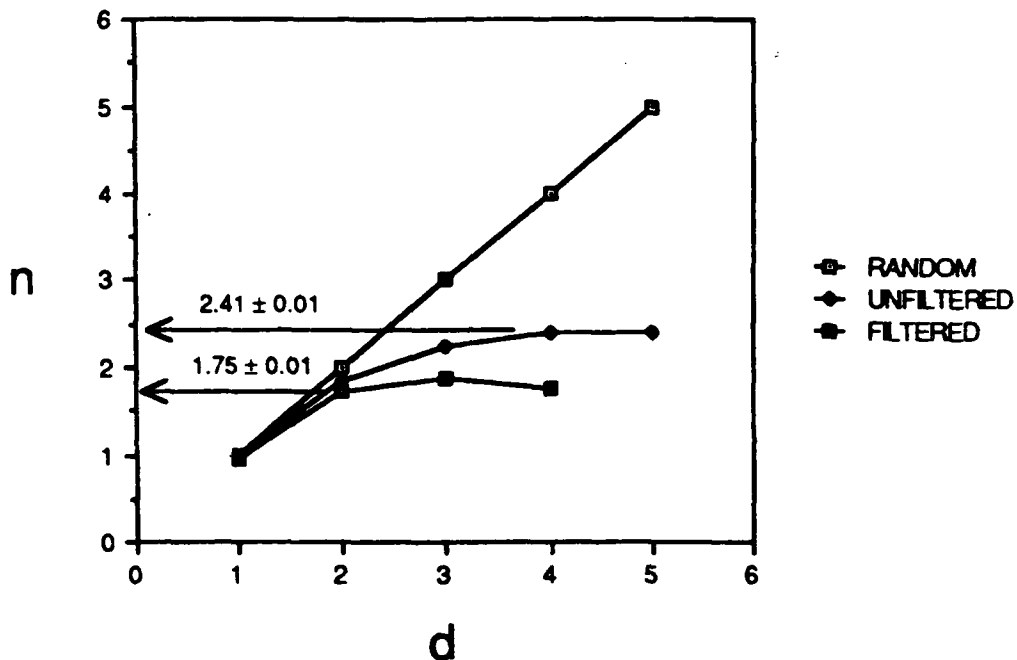
**Figure 10:** Integral autocorrelation functions of activity shown in Fig. 5 after interpolation at 0.1 sec intervals; unfiltered data. Calculations were conducted for embedding dimension  $d = 1$  through 5.



**Figure 11:** Determination of regions along curves of Fig. 10 having linear and saturating slopes.

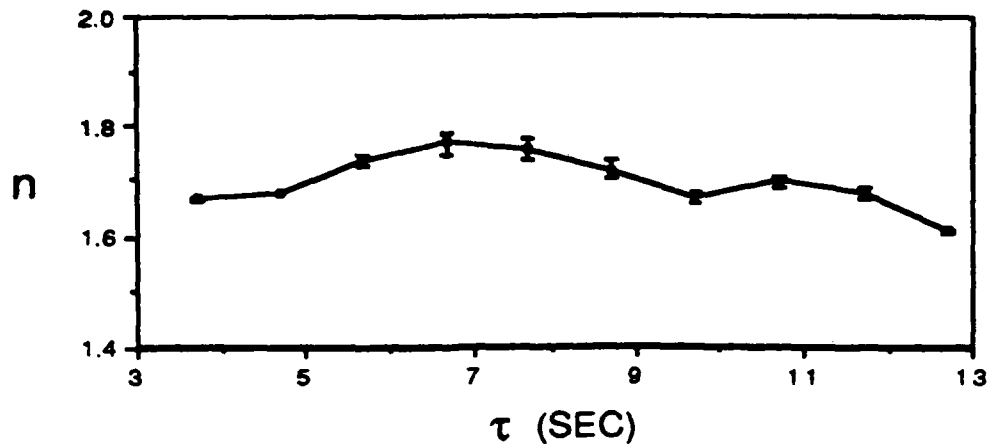
The slopes along the plots of  $\log C(r)$  versus  $\log (r)$  curves often show variability (Fig. 10). In order to estimate the appropriate regions at which the slopes are linear and saturate toward a common value, we followed the example of Rapp *et al.* [46] and calculated the slope of the curves between successive points. These slopes were then plotted against  $\log C(r)$  in Fig. 11. In the indicated range of Fig. 11, the points for  $d = 1, 2$  are easily distinguishable at the bottom near the  $\log C(r)$  axis, but those for  $d = 3, 4, 5$  intermingle. The indicated regions along the  $\log C(r)$  dimension were then used to calculate the slopes  $n$  along the same regions for each  $d$  in

Fig. 10. Figure 12 shows the results of plotting  $n$  against  $d$  for the unfiltered activity of the motoneuron. Also shown are the results for the filtered data of Fig. 6, and for random noise having the same number of points, mean, and standard deviation as in the motoneuron series. For random noise,  $n$  scaled linearly and equally with increasing  $d$ . The unfiltered data saturated at a fractal dimension above 2 at  $d = 4$ , whereas the filtered data saturated at a fractal dimension below 2 at  $d = 2$ . The error levels were quite low, being smaller than the points in the graph. Using selective filters, we found that it was the high-frequency components that produced the difference between the filtered and unfiltered saturation levels in Fig. 12.



**Figure 12:** Saturation of dimension  $n$  with increasing embedding dimension  $d$ . Unfiltered data saturated at  $d = 4$ , whereas the filtered data saturated at  $d = 2$ . Random noise did not saturate. Standard error for each calculation was smaller than the size of the symbol in the illustration. Curves are drawn through points in order to aid visualization. See Figs. 10 and 11.

The saturation values of  $n$  were quite stationary when examined with different scaling factors. Similar saturation levels were obtained with interpolation rates of 0.25 and 0.05 sec as with the 0.1 sec rate used above. In addition, as shown in Fig. 13 for the filtered and 0.1 interpolated data, the saturation levels were relatively unaffected by changing  $\tau$  in the calculations of  $C(r)$ . The average orbital period, as calculated from Poincaré sections of the phase portrait (discussed below), was 15 sec, and, therefore, the series of  $\tau$  shown in Fig. 13 properly covered a large range of the orbit time.



**Figure 13:** Topological dimension  $n$  remained stationary with increasing  $\tau$ ;  $d$  also remained constant, but is not shown here. Calculations were conducted on the filtered series shown in Fig. 6.

#### Lyapunov Exponents

Lyapunov exponents provide a means for determining the topological growth of the attractor as the time series evolves. We used the computer programs of Alan Wolf (personal communication) and Wolf, Swift, Swinney, and Vastano [55] to calculate the first Lyapunov exponent. Conceptually, the algorithm defines a  $d$ -dimensional sphere. Each dimension has a Lyapunov exponent ( $\lambda$ ) indicating the rate of growth of the attractor in that dimension. The sum of the exponents in a dissipative system is negative. Chaotic attractors have at least one positive exponent denoting exponential divergence of nearby trajectories; i.e., stretching occurs on the attractor in certain direction(s) of phase space (positive  $\lambda$ ), while contraction occurs in other directions (negative  $\lambda$ ). In systems having positive  $\lambda$ , folding must occur in order to keep the diverging trajectories within a bounded surface.

From Wolf et al. [55], the algorithm for determining  $\lambda_1$  is:

$$\lambda_1 = \frac{1}{t_M - t_0} \sum_{k=1}^M \log_2 \frac{L'(t_k)}{L(t_{k-1})} \quad (2)$$

The total time for evolving through data consisting of  $M$  equally spaced points is  $t_M$ , and  $t_0$  is the initial time.  $L(t_{k-1})$  is the distance separating a point on a fiducial trajectory of the attractor and a nearest point in phase space at time  $t_{k-1}$ .  $L'(t_k)$  is a new distance between the fiducial point and another nearest replacement point after the trajectory has evolved a prescribed number of steps to time  $t_k$ . As a simple example, one might start by determining the distance between two points lying in adjacent trajectories in Fig. 10. After evolving a number of time steps along a

trajectory, the distance between the points may have increased. After a series of similar iterations involving increasing replacement distances, the above equation yields a positive change in  $\lambda_1$  in bits per sec.

Two scaling factors critically influence the calculations of  $\lambda_1$ : the number of time steps in the evolution through the attractor before making the calculations, and the maximum distance through the range of the data in searching for the replacement points at each calculation. To determine the appropriate range for each of these scaling factors, we calculated  $\lambda_1$  for a series of evolution times and maximum replacement distances: First,  $\lambda_1$  was calculated for a given evolution time (multiple of the 0.1 sampling interval) and a series of maximum allowable replacement distances (percent of the range of the data). For each pair of evolution time and replacement distance, the calculations generated relatively stationary  $\lambda_1$  values as the iterations progressed through the time series (Fig. 14). Second, the stationary  $\lambda_1$  obtained for the series

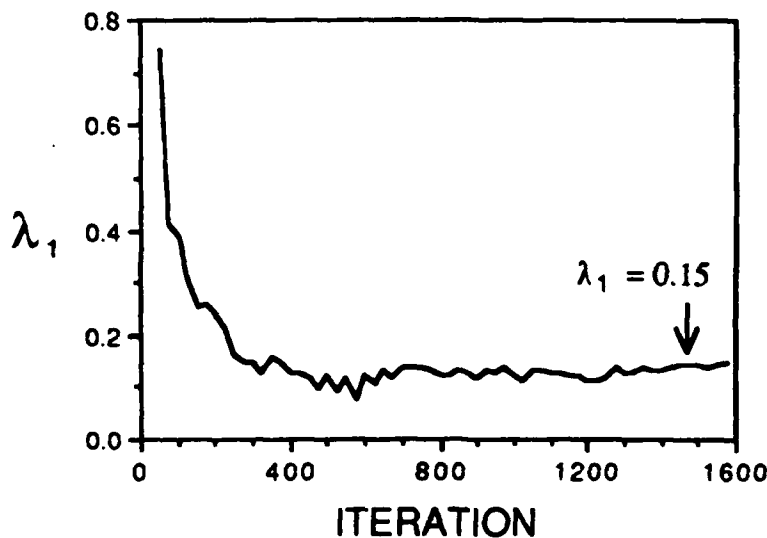


**Figure 14:** First Lyapunov exponent (in bits/sec). Calculations were made at fixed intervals (multiples of the sampling interval) in the evolution through the attractor. Note that the exponent reached a positive, stationary value. The embedding space was constructed using  $\tau = 3.7$  sec and  $d = 3$ .

of calculations with each evolve step was plotted against a range of maximum allowable replacement distances (Fig. 15). The results show that replacement distance  $L'_{\max}$  was a more critical factor than evolution time EVOLVE. For small replacement distances, different evolution

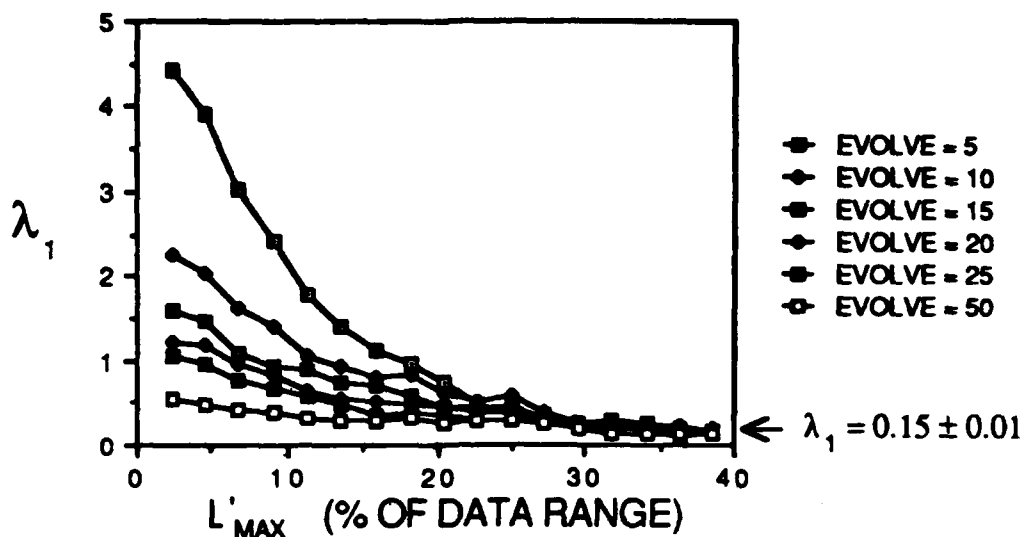


**Figure 15:** The first Lyapunov exponent plotted as a function of EVOLVE (multiples of the sampling interval) and  $L'_{MAX}$  (the maximum prescribed scaling through the range of the data before making each calculation). Embedding space here was constructed using  $\tau = 3.7$  sec and  $d = 3$ .

steps generated different  $\lambda_1$ , but for replacement distances of about 30% of the data range, all evolution steps generated similar  $\lambda_1$ . Using an EVOLVE of 20 and a maximum replacement distance of 30% of the data range, we also determined that  $\lambda_1$  was reasonably stationary over a wide range of  $\tau$  (Fig. 16).

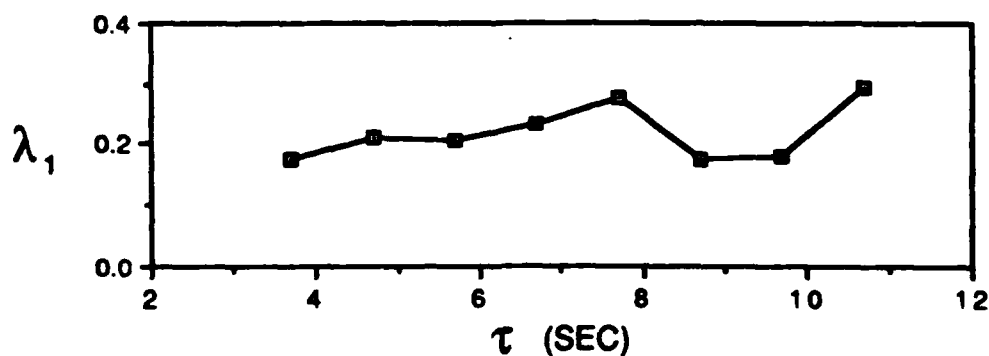


**Figure 16:** First Lyapunov exponent remained relatively stationary when the calculations were made in embedding space constructed with different lags  $\tau$ .

#### 1D Map

The trajectories representing the activity of the motoneuron that we have been analyzing have an unpredictable yet deterministic interrelationship with one another. To demonstrate

this, we first obtained a Poincaré cross section of the flow of the trajectories through phase space, and then constructed a 1D map of the relative position of the trajectories within the Poincaré section, much as Roux, Simoyi, and Swinney [49] have described in their analysis of the Belousov-Zhabotinskii reaction.

The horizontal line in Fig. 17A shows the level at which we made a cut in the 2-D phase portrait. The one-way crossings of the trajectories through this line yielded the average orbital period and the interrelationship of one trajectory to another. Each trajectory crossed the line at some parameter value and with an average period of 15 sec. We then normalized the parameter positions of the crossings and plotted them in Fig. 17B as a 1D map showing the relative position of a particular crossing ( $t_{n+1}$ ) with respect to the previous crossing ( $t_n$ ). The number next to each point in Fig. 17B shows which ordered-pair of Poincaré crossings the point represents.

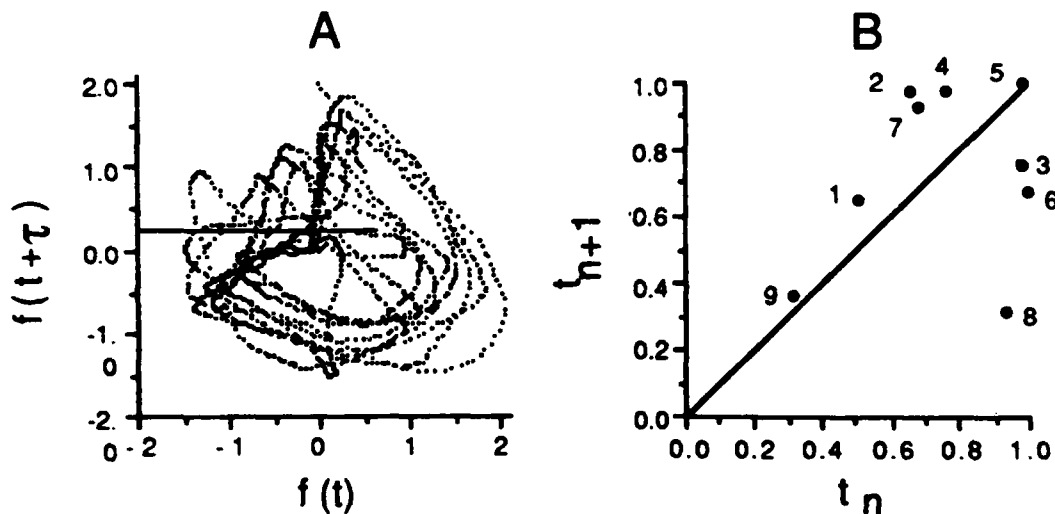


**Figure 17:** (A) Poincaré section was taken at the horizontal line through a 2-D phase portrait. (B) 1D map constructed by plotting the relative position of ordered pairs of trajectories passing in the same direction through the horizontal line. The numbers next to each point show the succession of ordered-pairs.

We can extract two important features from the 1D map. First, the points are not randomly scattered. In fact, they appear to fall on a relatively smooth curve having a positive slope above the 1:1 line and a very steep negative slope below the 1:1 line. Second, although there are not enough Poincaré crossings to define the exact slope of a smooth curve as it crosses the 1:1 line, the steepness of the fall-off below the line strongly suggests that the slope is greater than -1. Both of these findings are consistent with the findings we presented in the previous sections indicating that the activity of the motoneuron was chaotic: the nonrandom positions of the points show that the activity was governed by a deterministic process, and the steep fall-off

shows that the activity was not a limit cycle, but rather that it was unpredictable (nonperiodic). The shape of the series of points in Fig. 17B is similar to the 1D map in Chay's [9] computer studies in which she found that spiking activity of simulation neurons bifurcated from periodic activity into chaos through period doubling. One interesting difference, is that while both Chay's simulation study and our study dealt with single neurons, the simulations dealt solely with the generation of chaos in the interspike intervals, whereas our analyses dealt with the cycle of high-frequency bursts that comprised the motor pattern. Moreover, because the motoneuron was driven by BCNs, which generate the rhythmic pattern of activity [39], it seems likely that our results apply not only to chaos in a single motoneuron neurons but also to chaos reflecting the integrated activity of the group of coactive neurons. Examination of the activity in individual BCNs has demonstrated similar evidence of low-dimensional chaos as in the motoneurons.

#### MOTOR PATTERN HETEROGENEITY

In the above discussion we have examined variability occurring within a relatively homogeneous motor pattern. However, even in response to constant stimulation, motor patterns can be structurally nonhomogeneous. An example of this is shown in Fig. 18. The first

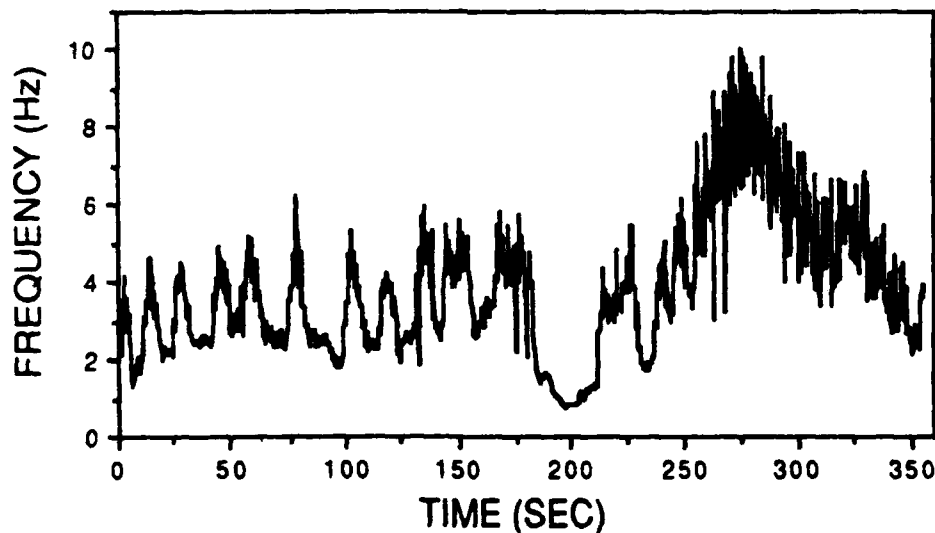


**Figure 18:** Heterogeneity of firing in a brain motoneuron. First half of the record is the same as in Fig. 5. Second half of the record, representing regurgitation behavior, arose spontaneously. The activating stimulus was the same throughout and consisted of brief (1 msec) electrical pulses that were applied at a rate of 1 Hz to the stomatogastric nerve, an afferent root of the buccal ganglion.

200 sec of this activity is the same as shown in Fig. 5. After that point, the repeating bursts increased rapidly and overlapped into a peak of high-frequency activity. Subsequently, as the overall frequency decreased, the individual bouts of high-frequency firing again reappeared.

During instances of alterations in the pattern of firing, some neurons become more active while others become more quiescent. The new motor pattern usually has a shorter duration than the one from which it emerges, and often has characteristics that resemble the motor pattern relating to the active phase of regurgitation [34,35,38]. Figure 19 shows a segment of a motor pattern involving three neurons that can be reidentified in successive preparations: the

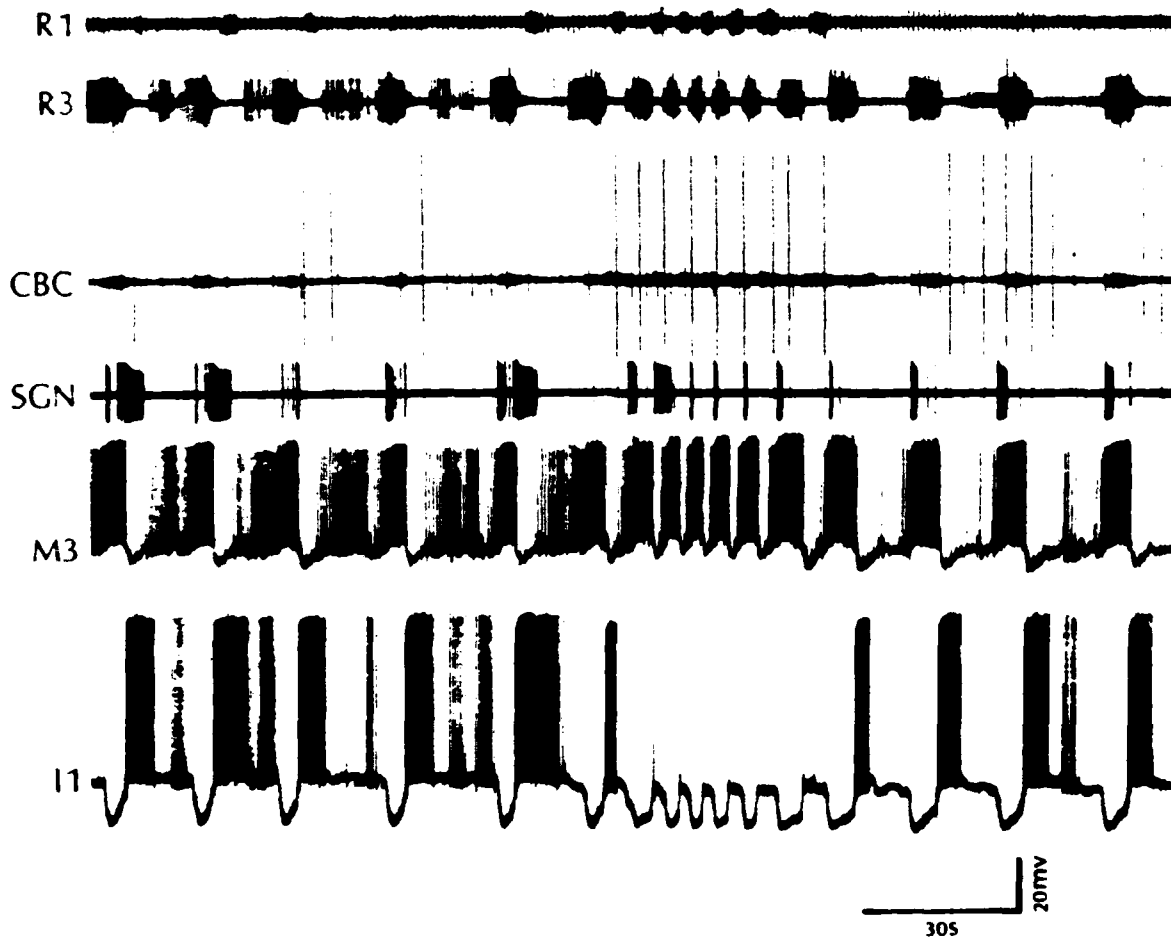


**Figure 19.** Heterogeneity of firing in many neurons. Note the spontaneous shift of activity, first, from a low-frequency pattern, which relates to bite-swallow behavior, to a higher-frequency pattern, which relates to regurgitation behavior, and then the return to the first. M3 is a reidentifiable buccal ganglion motoneuron, and I1 is a reidentifiable interneuron. SGN is the stomatogastric nerve which innervates the salivary gland, and CBC is the cerebral-buccal connective. Small-amplitude bursts in the CBC were primarily from the BCNs; large spike was from the metacerebral giant neuron in the brain. Tonic electrical pulses were applied to the SGN on the opposite side of the buccal ganglion. Other captions are the same as in Fig. 3.

metacerebral giant neuron (located in the brain) whose axon spike appears in the CBC trace of Fig. 19; a buccal ganglion motoneuron (trace M3), and a buccal ganglion interneuron (trace I1). The illustrated segment was taken from a 10 min recording, during which the pattern switched approximately every 90 sec. As in the case observed in recordings taken from relatively intact animals [38], some episodes of motor pattern switching were often composed of blends of the two extremes shown in Figs. 18 and 19. As we shall discuss, such motor pattern variations pose difficult though interesting problems in the application of dynamical theories to behavior.

## DISCUSSION

In order to focus explicitly on variability arising from processes within the central nervous system, we used nervous systems that had been completely removed from sensory inputs and motor effectors. Such isolated nervous systems have been characterized previously [e.g., 14,34-36,39]. In this chapter we have analyzed the activity of a motoneuron which received inputs from several BCNs that are responsible for generating and controlling rhythmic motor output underlying different behaviors. The neurophysiological records that we chose to analyze had characteristics that posed problems, as presented above, that neurobiologists often face in experimental situations. Despite these problems, the results appear to be relatively robust. In further work, we have analyzed the activity of other motoneurons and BCNs, some of whose activity was considerably longer than the present example, and have obtained similar results.

### Chaotic Attractors in the Generation of Motor Patterns

Evidence for presence of chaotic attractors. The definition of attractors has been widely discussed [e.g., 1,12,15,30,53]. In reference to neural networks, they may be considered simply as energy states that form and constrain the integrated activity within a limited parameter space defined by the phase portrait. The conclusion that the attractors in *Pleurobranchaea* may be chaotic follows from the findings that: 1) Autocorrelation functions quickly fall to zero. 2) Calculation of correlation dimensions shows that the activity is governed by fractal topological structures that are embedded in low-dimensional state space. 3) Trajectories in the phase portraits appear to diverge from one another. This finding is supported by calculations showing that the first Lyapunov exponent is positive which indicates that the trajectories diverge exponential, and that there must be folding of the attractor in order to keep the trajectories within a bounded surface. 4) 1D maps taken from Poincaré sections show that the interrelated positions of the trajectories are not random, but, rather, appear to follow some relatively simple function whose structure is indicative of nonperiodic behavior. These findings indicate that the pattern-generating mechanisms in *Pleurobranchaea* themselves generate unpredictable

though deterministic activity in the same way that mathematical relationships such as the logistic equation [32] or the Rössler attractor [48] generate chaotic or unpredictable activity.

Behavior-specific chaotic attractors. Previous analyses of repetitive behavior or oscillatory brain function have fruitfully characterized the dynamics of repetitive behavior, or of the underlying neural activity, as limit cycles [21-23,25,45]. In rabbit olfactory EEGs, basal chaotic activity provides a route for limit cycles to emerge that represent particular odors [12,53]. Similarly, "critical fluctuations" have been proposed as a means by which phase transitions occur in human hand and finger movements [22]. Chaotic activity may also provide a route for pattern switching in *Pleurobranchaea*. However, the predominance of evidence for chaos in our records suggests that chaotic attractors themselves may be behavior-specific. Although chaos has been proposed to occur in a variety of biological systems [3-5,12,27,33,50,53], to our knowledge the work reported here constitutes the first evidence of chaos in patterned activity that is relatable to adaptive behavior in whole animals.

#### Nonstationary Motor Patterns

Intrinsic variation and adaptive stability. By being sensitive to initial conditions, a signal exhibiting intrinsic variation, in contrast to a nonvarying signal or one on which extrinsic noise is superimposed, can carry new information into the future. The intrinsic variations that we have ascribed above to chaos, represent in effect the attempt of the nervous system to generate new informational space which, we propose, provides for stability in the animal's adaption to a varying and often unpredictable environment.

In the natural environment, animals are often confronted by many stimuli simultaneously requiring a "behavioral choice" to respond selectively [10] or to exhibit a blend [6,28,29,38]. Considered from a classical perspective, there may be reflex interactions between separate neurocircuits relating to the different behaviors [26]. However, even given evidence of such reflex interactions, a view of the "neurocircuit" as arising from self-organizing cooperativity among groups of neurons, as defined in the Introduction, may give some insight into the spontaneous pattern switching and blending that we have presented above in reference to Figs. 18 and 19.

Consider the following example: inverted animals exhibit slower righting behavior when food is present than when there is no food [10]. In order to right themselves, animals usually have to twist the anterior portion of the foot, but they also direct the foot toward the direction of the food stimulus (Fig. 1) and may even try to "grasp" it. Thus, when animals are inverted and presented food, the neurons governing the movement of the anterior regions of the foot may receive instructions simultaneously for two different behaviors. Such influxes of mixed sensory instructions may lead to the production of hybrid or blended behaviors, and thereby cause an

increase in the execution time (or complete suppression) of one or both behaviors, not so much by reflex inhibition of one behavior to another, but more because of a lack of sufficient "consensus" of information arising among the converging sensory inputs as they compete for activation of target neurons. Because the buccal-oral system of *Pleurobranchaea* has a greater range of multifunctional capabilities than the foot, and because the BCNs are key elements in the generation and control of all of these behaviors [39], it is not surprising that blends of motor patterns should be observed in the activity of the BCNs and in the neurons with which they interact.

Adaptive attractors and blending. The present findings lead to two interrelated questions that pose difficult experimental problems: 1) If neural output is so variable and unpredictable, what determines the appropriate response? 2) Can the attractor concept account for blending? In response to the first question, we propose that there may be no appropriate centrally programmed motor pattern or genetically established neurocircuit for a behavior [38,39]. Rather, the self-organizing process can lead to many types of motor patterns, some of which may be nonadaptive for the particular conditions surrounding the animal. The correct motor pattern and the effective "neurocircuit" arise from continual dialectic interactions between the animal and the environment. Variability occurring naturally in the *Pleurobranchaea* nervous system gives these emerging "neurocircuits" a fluid quality. The interaction of the animal with the environment further accentuates such fluidity. It is necessary, therefore, to consider the combined effects of two sources of influence, one intrinsic and the other extrinsic, in the process by which functional neurocircuits emerge during the production of adaptive behavior.

In response to the second question, the advantage of state space analyses and attractor formulations is that many quantitative features of dynamical processes may be obtained without having to determine the equations of motion. However, the apparent fluidity of neural activity poses difficulties in applying dynamical theories. For example, nonhomogeneous attractors that have topological features representing different types of motor patterns may be appropriate when the patterns represent different aspects of the same behavior, but are more difficult to invoke in order to account for the appearance of different behaviors. It is probably more useful to consider motor pattern switching (Figs. 18 and 19) as bifurcations from an attractor to another, with each attractor representing a different behavior or motor pattern. Since the entire phase space represents the possible dynamical combinations of the group of coactive neurons, it is not unreasonable that intermediate areas between the attractors, or the basins of individual attractors, could have mixtures of several motor patterns. An interesting possibility is that the attractors themselves may not be stationary and that together the different attractors are part of a larger, "hyper" attractor having its own dynamics.

Unlike known mathematical and physical attractors that have stationary qualities, neural systems are subject to many temporal changes that alter the underlying framework from which the patterns emerge. There may be long-term effects relating to learning or hormone levels, but short-term effects are probably more common. Examples of short-term effects were shown in Figs. 3 and 4 regarding the effect of history on the generation of motor patterns. Given a quiescent nervous system or a recent startup of a particular motor pattern, the activity may appear as shown for the first sections of Fig. 18 and 19. As the activity progresses, the underlying context of group activity may change because individual neurons are affected by the preceding activity in which they take part. As each neuron changes, its parametric effect on the group can also change. Depending on the extent of such parametric changes, the activity of the group may show reversible temporal fluctuations and graded shifts into new types of activity.

### CONCLUSION

We have attempted to illustrate in this chapter that functional "neurocircuits" leading to adaptive behavior have a fluid quality. In order for concepts such as attractors to be useful they must be able to account for these fluid qualities. While these constructs, which have arisen primarily from studies in the dynamics of idealized physical and mathematical models, have been useful in the study of variability in our experimental system, the experimental system in turn seems to pose questions for further development of dynamical theory. Although we have examined the possibility that there may be chaos in neural processing, our central question has not so much to do with chaos *per se*, but rather with the role of variation and of the types of variations that become involved in the emergence of self-organization. Moreover, inasmuch as nervous systems (as most biological systems) are distributed, parallel, variable, self-organizing, and dialectical, it is essential, as discussed with regard to the neural basis of learning [40,41], to develop a conceptual language for addressing these issues more effectively than present theory allows. Inasmuch as our experimental system is not unique in its essential characteristics, comparative analyses of such relatively "simple" systems may help to uncover general principles underlying the self-organization of activity in cooperative groups.

### ACKNOWLEDGEMENTS

We thank Al Albano, Robert Burton, John Edstrom, Paul Rapp, William Shaffer, Alan Wolf, and David Zopf for helpful discussions. We are especially grateful to Alan Wolf for letting us use his computer programs to calculate Lyapunov exponents, and to Lavern Weber for the generous use of facilities at the Hatfield Marine Science Center.

## REFERENCES

1. Abraham, R. H., and C. D. Shaw (1983) Dynamics--The Geometry of Behavior, Parts 1-4, Aerial Press, Santa Cruz.
2. Ayers, J., G. Carpenter, S. Currie, and J. Kinch (1983) Which behavior does the lamprey central motor program mediate? *Science* **221**: 1312-1315.
3. Aihara, K., and G. Matsumoto (1986) Chaotic oscillations and bifurcations in squid giant axons. In Chaos, A. V. Holden, ed., pp. 257-269, Princeton University Press, Princeton.
4. Babloyantz, A., and A. Destexhe (1986) Low-dimensional chaos in an instance of epilepsy. *Proc. Natl. Acad. Sci. USA* **83**: 3513-3517.
5. Babloyantz, A., J. M. Salazar, and C. Nicolis (1985) Evidence of chaotic dynamics of brain activity during the sleep cycle. *Phys. Lett.* **111A**: 152-155.
6. Bellman, K. L. (1979) The conflict behavior of the lizard, *Sceloporus occidentalis*, and its implication for the organization of motor behavior. PhD Dissertation. La Jolla, CA: University of California, San Diego.
7. Bullock, T. H. (1980) Reassessment of neural connectivity and its specification. In Information Processing in the Nervous System, H. M. Pinsky and W. D. Willis, eds., pp. 199-220, Jr. Raven Press, New York.
8. Carew, T. J., and C. L. Sahley (1986) Invertebrate learning and memory: From behavior to molecules. *Ann. Rev. Neurosci.* **9**: 435-487
9. Chay, T. R. (1985) Chaos in a three-variable model of an excitable cell. *Physica* **16D**: 233-242.
10. Davis, W. J., G. J. Mptsois, and M. Pinneo (1974) The behavioral hierarchy of the mollusk *Pleurobranchaea*. I. The dominant position of the feeding behavior. *J. Comp. Physiol.* **90**: 207-224.
11. DiDominico, R., and R. C. Eaton (1985) Seven principles for command and the neural causation of behavior. *Brain Behav. Evol.* In press.
12. Freeman, W. J., and C. A. Skarda (1985) A perspective on brain theory: Nonlinear dynamics of neural masses. *Brain Res. Rev.* **10**: 147-175.
13. Getting, P. A., and M. S. Dikin (1985) *Tritonia* swimming: A model system for integration within rhythmic motor systems. In Model Neural Networks and Behavior, A. I. Selverston, ed., pp. 3-20, Plenum Press, New York.
14. Gillette, R., M. Kovac, and W. J. Davis (1978) Command neurons in *Pleurobranchaea* receive synaptic feedback from the motor network they excite. *Science* **199**: 798-801.
15. Grassberger, P., and I. Procaccia (1983) Characterization of strange attractors. *Phys. Rev. Lett.* **50**: 346-349.
16. Grossberg, S. (1980). Studies of Mind and Brain. Reidel Publishing Co. Boston.

17. Haken, H. (1983). Synergetics: An Introduction. Nonequilibrium Phase Transitions and Self-Organization in Physics, Chemistry, and Biology. 3rd Edn., Springer-Verlag, New York.
18. Harmon, L. (1964) Neuromimes: Action of a reciprocally inhibitory pair. *Science* **146**: 1323-1325.
19. John, E. R. (1972). Switchboard versus statistical theories of learning and memory. *Science* **177**: 850-864.
20. Katchalsky, A., V. Rowland, and R. Blumenthal (1974) Dynamic patterns of brain cell assemblies. *Neurosci. Res. Prog. Bull.* **12**: 3-187.
21. Kelso, J. A. S., E. L. Saltzman, and B. Tuller (1986a) The dynamical perspective on speech production: Data and theory. *J. Phonet.* **14**: 29-59.
22. Kelso, J. A. S., Scholz, J. P., and G. Schöner (1986) Nonequilibrium phase transitions in coordinated biological motion: Critical fluctuations. *Phys. Lett.* **118A**: 279-284.
23. Kelso, J. A. S., and B. Tuller (1986) A dynamical basis for action systems. In Handbook of Cognitive Neuroscience, M.S. Gazzaniga, ed., pp. 321-356, Plenum Press, New York.
24. Kennedy, D., and W. J. Davis (1977) Organization of invertebrate motor systems. In Handbook of Physiology, Vol. 2: Neurophysiology, 2nd Edition, E. R. Kandel, ed., pp. 1023-1087, American Physiological Society, Bethesda.
25. Kopell, N. (1987) Toward a theory of modelling central pattern generators. In Neural Control of Rhythmic Movements, A. H. Cohen, S. Rossignol, and S. Grillner, eds., John Wiley and Sons, Inc., New York. In press.
26. Kovac, M. P., and W. J. Davis (1980) Reciprocal inhibition between feeding and withdrawal behaviors in *Pleurobranchaea*. *J. Comp. Physiol.* **139**: 77-86.
27. Mackey, M. C., and L. Glass (1977) Oscillation and chaos in physiological control systems. *Science* **197**: 287-289.
28. Leonard, J. L., and K. Lukowiak (1985) The forms of spontaneous and evoked gill movements in *Aplysia*. *Soc. Neurosci. Abstr.* **11**: 191.7.
29. Leonard, J. L., J. Edstrom, and K. Lukowiak (1987) A re-examination of the "gill withdrawal reflex" of *Aplysia californica* Cooper (Gastropoda: Opisthobranchia). Preprint.
30. Mandelbrot, B. B. (1985) The Fractal Geometry of Nature, Freeman & Co., New York.
31. Marder, E. and S. L. Hooper (1985) Neurotransmitter modulation of the stomatogastric ganglion of decapod crustaceans. In Model Neural Networks and Behavior, A. I. Selverston, ed., pp. 319-338, Plenum Press, New York.
32. May, R. M. (1976) Simple mathematical models with complicated dynamics. *Nature* **261**: 459-467.
33. Markus, M., D. Kuschmitz, and B. Hess (1985) Properties of strange attractors in yeast glycolysis. *Biophys. Chem.* **22**: 95-105.

34. McClellan, A. D. (1980) Feeding and regurgitation in *Pleurobranchaea californica*: Multibehavioral organization of pattern generation and higher order control. Ph.D. thesis. Case Western Reserve University, Cleveland, Ohio
35. McClellan, A. D. (1982) Movements and motor patterns of the buccal mass of *Pleurobranchaea* during feeding, regurgitation, and rejection. *J. Exp. Biol.* 98: 195-211.
36. McClellan, A. D. (1982) Re-examination of presumed feeding motor activity in the isolated nervous system of *Pleurobranchaea*. *J. Exp. Biol.* 98: 212-228.
37. McDougall, W. (1903) The nature of inhibitory processes within the nervous system. *Brain* 26: 153-193.
38. Mpitsos, G. J., and C. S. Cohan (1986) Comparison of differential Pavlovian conditioning in whole animals and physiological preparations of *Pleurobranchaea*: Implications of motor pattern variability. *J. Neurobiol.* 17: 499-516.
39. Mpitsos, G. J., and C. S. Cohan (1986) Convergence in a distributed motor system: Parallel processing and self-organization. *J. Neurobiol.* 17: 517-545.
40. Mpitsos, G. J., S. D. Collins, and A. D. McClellan (1978) Learning: A model system for physiological studies. *Science* 199: 497-506.
41. Mpitsos, G. J., and K. Lukowiak (1985) Learning in gastropod molluscs. In The Mollusca. A. O. D. Willows, ed., pp. 95-267, Academic Press, New York.
42. Nolen, T. G., and R. R. Hoy (1984) Initiation of behavior of single neurons: The role of behavioral context. *Science* 226: 992-994.
43. Packard, N. H., J. P. Crutchfield, J. D. Farmer, and R. S. Shaw (1980) Geometry from a time series. *Phys. Rev. Lett.* 45: 712-716.
44. Perkel, D., and B. Mulloney (1974) Motor pattern production in reciprocally inhibitory neurons exhibiting inhibitory rebound. *Science* 185: 181-183.
45. Rand H., A. H. Cohen, and P. J. Holmes (1987) Systems of coupled oscillators as models of CPG's. In *Neural Control of Movements in Vertebrates*, A. H. Cohen, S. Rossignol, and S. Grillner, eds., Wiley and Sons, New York. In press.
46. Rapp, P. E., I. D. Zimmerman, A. M. Albano, G. C. Deguzman, and N. N. Greenbaun (1985) Dynamics of spontaneous Neural activity in the simian motor cortex: The dimension of chaotic neurons. *Phys. Lett.* 110A: 335-338.
47. Ritzmann, R. E., M. L. Tobias, and C. R. Fournier (1980) Flight activity initiated by giant interneurons of the cockroach: Evidence for bifunctional trigger interneurons. *Science* 210: 443-445.
48. Rössler, O. E. (1979) An equation for continuous chaos. *Phys. Lett.* 57A: 397-398.
49. Roux, J.-C., R. H. Simoyi, and H. L. Swinney (1983) Observation of a strange attractor. *Physica* 8D: 257-266.
50. Schaffer, W. M., S. Ellner, and M. Kot (1986) Effects of noise on some dynamical models in ecology. *J. Math. Biol.* 24: 479-523.

51. Schönner, G., H. Haken, and J. A. S. Kelso (1986). A stochastic theory of phase transitions in human hand movement. *Biol. Cybern.* 53: 1-11.
52. Shaw, R. (1986) The Dripping Faucet. Aerial Press, Santa Cruz.
53. Skarda, C. A., and W. J. Freeman (1987) How brains make chaos in order to make sense of the world. *Behav. Brain Sci.* 10: 161-195
54. Takens, F. (1981) Detecting strange attractors in turbulence. In Lecture Notes In Mathematics, Vol. 898. D. A. Rand and L. S. Young, eds., pp. 366-381, Springer-Verlag, Berlin.
55. Wolf, A., J. B. Swift, H. L. Swinney, and J. A. Vastano (1985). Determining Lyapunov exponents from a time series. *Physica* 16D: 285-317.